

# Spin liquid to spin glass crossover in the random quantum Heisenberg magnet

Maine Christos,<sup>1</sup> Felix M. Haehl<sup>2</sup>, and Subir Sachdev<sup>1,2</sup>

<sup>1</sup>*Department of Physics, Harvard University, Cambridge Massachusetts 02138, USA*

<sup>2</sup>*School of Natural Sciences, Institute for Advanced Study, 1 Einstein Drive, Princeton, New Jersey 08540, USA*



(Received 18 October 2021; accepted 26 January 2022; published 14 February 2022)

We study quantum  $SU(M)$  spins with all-to-all and random Heisenberg exchange interactions of root-mean-square strength  $J$ . The  $M \rightarrow \infty$  model has a quantum spin liquid ground state with the spinons obeying the equations of the Sachdev-Ye-Kitaev (SYK) model. Numerical studies of the  $SU(2)$  model with  $S = 1/2$  spins show spin glass order in the ground state, but also display SYK spin liquid behavior in the intermediate frequency spin spectrum. We employ a  $1/M$  expansion to describe the crossover from fractionalized fermionic spinons to a confining spin glass state with weak spin glass order  $q_{EA}$ . The SYK spin liquid behavior persists down to a frequency  $\omega_* \sim Jq_{EA}$ , and for  $\omega < \omega_*$ , the spin spectral density is linear in  $\omega$ , thus quenching the extensive zero temperature entropy of the spin liquid. The linear  $\omega$  spectrum is qualitatively similar to that obtained earlier using bosonic spinons for large  $q_{EA}$ . We argue that the extensive SYK spin liquid entropy is transformed as  $T \rightarrow 0$  to an extensive complexity of the spin glass state. We comment on holographic connections of the confinement transition to the fragmentation of black holes with  $AdS_2$  horizons.

DOI: [10.1103/PhysRevB.105.085120](https://doi.org/10.1103/PhysRevB.105.085120)

## I. INTRODUCTION

A common theme in many experimental studies of the hole-doped cuprate compounds below optimal doping is that while there is nearly static spin or charge order at low temperatures, the intermediate temperature pseudogap regime can be described in terms of an underlying quantum spin liquid state. Among recent studies, we note the nuclear magnetic resonance observations in  $La_{2-x}Sr_xCuO_4$  of Frachet *et al.* [1] showing spin glass order at low temperature all the way up to optimal doping; the neutron scattering observations of Ma *et al.* [2] on  $La_{1.6-x}Nd_{0.4}Sr_xCuO_4$  showing spin stripe order at low temperature under the entire superconducting dome; and photoemission measurements [3,4] and angle-dependent magnetoresistance observations [5] in the pseudogap metal showing evidence for the breakdown of the Luttinger Fermi surface, which can be interpreted in terms of a fractionalized Fermi liquid containing a background quantum spin liquid [6,7]. In the undoped antiferromagnet, we recall the observations of Dalla Piazza *et al.* [8] showing intermediate energy spinon continua at wave vector  $(\pi, 0)$  in a system with long-range Néel order at wave vector  $(\pi, \pi)$ .

In this paper, we will study a random quantum Heisenberg magnet with all-to-all exchange interactions  $J_{ij}$

$$H = \frac{1}{\sqrt{N}} \sum_{i<j=1}^N J_{ij} \mathbf{S}_i \cdot \mathbf{S}_j. \quad (1.1)$$

We study an ensemble of models, where the  $J_{ij}$  are independent random variables for each pair  $(i, j)$ , and their ensemble averages are

$$\overline{J_{ij}} = 0, \quad \overline{J_{ij}^2} = J^2. \quad (1.2)$$

This model generalizes the classical Sherrington-Kirkpatrick model with Ising spins  $\sigma_i = \pm 1$  to quantum  $SU(2)$  spins  $\mathbf{S}_i$ , acting on a Hilbert space of states with angular momentum  $S = 1/2$  on each site.

Although such a random exchange model is far from the microscopic situation in the cuprates, it can successfully capture many aspects of cuprate phenomenology [9]. Here, we will show that it exhibits a deconfinement-to-confinement crossover, and we will obtain explicit results for the dynamic spin susceptibility across this crossover. This is one of the rare instances in which fractionalization and subsequent confinement can be described in a strongly coupled system with gapless matter.

The generalization of the model (1.1) to  $SU(M)$  spins, and the limits  $N \rightarrow \infty$  followed by  $M \rightarrow \infty$ , yield a fractionalized quantum spin liquid ground state [10] whose fermionic spinons obey the same equations as the complex Sachdev-Ye-Kitaev (SYK) model [11–14]. On the other hand, numerical studies [15–17] of the  $N \rightarrow \infty$  limit of the model (1.1) for  $SU(2)$  and spin  $S = 1/2$  show the presence of spin glass order in the ground state (in contrast to the SYK model itself, which does not have spin glass order [18]). However, the recent numerical study of the  $S = 1/2$   $SU(2)$  model argued [17] that the spin spectral density at intermediate frequencies matched that of the SYK spin liquid. Specifically, they observed

$$\chi''(\omega) \sim \frac{\text{sgn}(\omega)}{J} \left[ 1 - \frac{c}{J} |\omega| \dots \right], \quad \omega_* < |\omega| \ll J, T = 0. \quad (1.3)$$

The leading term in (1.3) has its origins in the spinons obeying the SYK equations [10]; it is often called the ‘marginal’ spectrum, because electrons scattering off such spin fluctuations acquire a marginal Fermi liquid Green’s function.

(The subleading term, with positive coefficient  $c$ , is related to the coefficient of the Schwarzian effective action [14].) Neutron scattering observations [2] on  $\text{La}_{1.6-x}\text{Nd}_{0.4}\text{Sr}_x\text{CuO}_4$  yield a momentum-integrated inelastic spin spectrum which is doping-independent, with some similarities to (1.3), along with a doping-dependent static spin stripe order; these features are similar to the numerical results on the random  $t$ - $J$  model [17], with the spin glass order replacing the spin stripe order.

A marginal spectrum is also obtained in the density fluctuations in a model with density-density interactions, and this has been argued [19] to be related to the anomalous continuum observed in dynamic charge response measurements [20,21] on optimally doped  $\text{Bi}_{2.1}\text{Sr}_{1.9}\text{Ca}_{1.0}\text{Cu}_{2.0}\text{O}_{8+x}$  (Bi-2212) using momentum-resolved electron energy-loss spectroscopy (M-EELS).

In the present paper, we will obtain an estimate of the low frequency bound  $\omega_*$  of the marginal spectrum, and also describe the nature of the crossover at  $\omega \sim \omega_*$ . This paper addresses the nature of the crossover from the spectrum in (1.3) to frequencies  $\omega < \omega_*$ . The presence of spin glass order implies a delta function at zero frequency

$$\frac{T\chi''(\omega)}{\omega} = \pi q_{EA} \delta(\omega), \quad (1.4)$$

where  $q_{EA}$  is the spin glass order parameter. We find that the crossover occurs at a frequency

$$\omega_* = Jq_{EA}, \quad \text{for } q_{EA} \ll 1, \quad (1.5)$$

and for smaller frequency

$$\chi''(\omega) = \frac{\omega}{\omega_*\pi J} + \dots, \quad 0 < |\omega| < \omega_*, \quad T = 0. \quad (1.6)$$

Given the numerical estimate  $q_{EA} \sim 0.02$  [17], the quantum spin liquid behavior of (1.3) is visible over a wide range of frequencies.

We note that a linear spectrum, qualitatively similar to (1.6), was found in an earlier theory [22,23] of the spin fluctuations by bosonic spinons. The bosonic spinon theory is valid for large  $S$ , and so leads to a large  $q_{EA}$  (see Appendix A); it also requires an additional assumption of marginal stability of a replica symmetry breaking solution to obtain the gapless spectrum. Our analysis uses fermionic spinons, does not require any additional marginal stability criteria, and is applicable for small  $q_{EA}$ . It is reassuring that the same qualitative behavior is obtained by fermionic and bosonic spinons. Thus we have a ‘‘duality’’ between fermionic and bosonic spinons present not only in the gapless, fractionalized, spin liquid regime [10], but also in the crossover to the confining spin glass state. We note that boson-fermion dualities have seen much discussion in the context of disorder-free gapless spin liquids on the square lattice [24,25].

At nonzero temperature, our results have interesting implications for the temperature dependence of the entropy, as sketched in Fig. 1.

The fractionalized SYK spin liquid has an extrapolated entropy which is extensive at  $T = 0$  [23]. The  $\text{SU}(2)$  model in (1.1) has a phase transition to a spin glass state with  $q_{EA} \neq 0$  at a small temperature  $T_{sg}$ , which is estimated in (4.19) in the  $\text{SU}(M \rightarrow \infty)$  limit. Below  $T_{sg}$  the entropy decreases so that there is no extensive entropy at  $T = 0$ . This spin glass

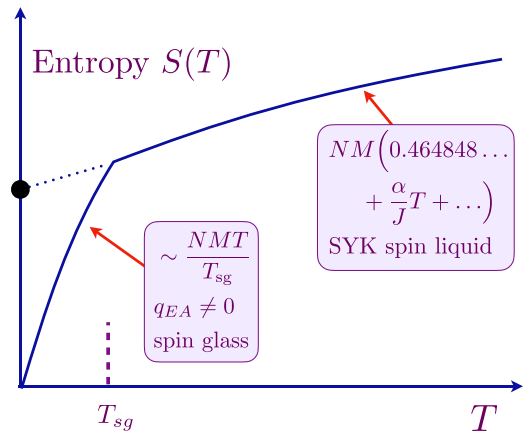


FIG. 1. Schematic plot of the temperature dependence of the entropy. There is a phase transition at  $T_{sg}$ . The  $\alpha$  coefficient is related to the coefficient of the Schwarzian in the theory of the spin liquid. We argue that the extrapolated  $T = 0$  entropy of the spin liquid (denoted by the filled circle) turns into the complexity of the spin glass by the fragmentation of phase space into an exponentially large number of disconnected sectors at temperatures below  $T_{sg}$ .

entropy should be interpreted as the entropy of quantum and thermal fluctuations within a given sector of phase space. However, the spin glass state also has a large number,  $e^{N\Sigma}$ , of disconnected sectors measured by the exponential of the complexity  $\Sigma$  [26–31]. We will estimate  $\Sigma$  for our quantum model here, and find that it remains nonzero as  $T \rightarrow 0$ . So we conclude that as we increase  $T$  past  $T_{sg}$ , the sectors reconnect, and the complexity turns into the quantum entropy of the SYK spin liquid.

The SYK spin liquid has a holographic description in terms of the  $\text{AdS}_2$  horizons of charged black holes [11,32,33]. Interestingly,  $\text{AdS}_2$  horizons have a fragmentation instability [34], and this has been connected to the physics of spin glasses [31,35–37]. The spin glass transition in Fig. 1 is therefore an instance of this instability of  $\text{AdS}_2$ : the fact that the spin glass state has vanishing zero temperature entropy implies that the instability can proceed to completion to a state without black hole horizons. Indeed, the instability of  $\text{AdS}_2$  depends upon the ultra-violet completion of the quantum gravity theory: it is not present for the SYK model [18], but is present for the  $\text{SU}(2)$  spin model in (1.1).

We will begin in Sec. II by formulating the path integral of the random  $\text{SU}(M)$  magnet for large  $N$  but general  $M$ . This will be a  $G$ - $\Sigma$ - $Q$  theory, involving a path integral over the fermionic spinon Green’s function and self energy,  $G$ ,  $\Sigma$ , and the spin autocorrelation  $Q$ . We will present the  $M \rightarrow \infty$  limit of this theory in Sec. III, which yields the quantum spin liquid state of Ref. [10]. Spin glass order is absent at  $M = \infty$ , but is present at any finite  $M$  because of a logarithm-squared divergence of the spin glass susceptibility [23]. We will describe such finite  $M$  effects in Sec. IV, and present the structure of the effective action for  $q_{EA}$  and the spin autocorrelation function in powers of  $1/M$ . Section V combines our results to obtain the feedback of the spin glass order on the dynamic spin spectrum. The low temperature complexity of the quantum spin glass state is discussed in Sec. VI.

## II. LARGE $N$ ACTION

All our analysis will be carried out in the  $N \rightarrow \infty$  limit of a model with  $SU(M)$  symmetry. We will keep  $M$  arbitrary in the present section. We consider the  $SU(M)$  spin model

$$H = \frac{1}{\sqrt{NM}} \sum_{i < j=1}^N \sum_{\alpha, \beta=1}^M J_{ij} S_{\beta}^{\alpha}(i) S_{\alpha}^{\beta}(j) \quad (2.1)$$

where  $S_{\beta}^{\alpha}(i) = [\mathcal{S}_{\beta}^{\alpha}(i)]^{\dagger}$  are generators of  $SU(M)$  on each site  $i$ , with  $\alpha, \beta = 1, \dots, M$ . Each site contains states corresponding to the *antisymmetric* product of  $kM$  (integer) fundamentals, and these are realized by fermionic spinons with

$$S_{\beta}^{\alpha}(i) = f_{\beta}^{\dagger}(i) f_{\alpha}(i) - k \delta_{\beta}^{\alpha}, \quad \sum_{\alpha} f_{\alpha}^{\dagger}(i) f_{\alpha}(i) = kM \quad (2.2)$$

with fermions  $f_{\alpha}(i)$  on each site  $i$ ; the model with bosons on each site realized the *symmetric* product of fundamentals, and is briefly discussed in Appendix A. Note that (2.2) implies that the spinons carry a  $U(1)$  gauge charge, where the gauge transformation can depend upon the site index  $i$ , and on time; such a gauge invariance is not present in the SYK model. However, the SYK model does have an emergent gauge symmetry involving gauge transformations that depend only on time (see Appendix B). We have made the spin operators traceless, and will restrict ourselves to the particle-hole symmetric case  $k = 1/2$ . The Hamiltonian in (2.1) reduces to the  $S = 1/2$  case of the  $SU(2)$  Hamiltonian in (1.1) for  $M = 2$  and  $k = 1/2$  (apart from an overall factor of  $1/\sqrt{2}$ ).

We introduce replicas  $a = 1, \dots, n$ , and average over  $J_{ij}$  to obtain the averaged, replicated partition function

$$\begin{aligned} \overline{\mathcal{Z}^n} &= \int \mathcal{D}f_{\alpha}^{\dagger}(i, \tau) \mathcal{D}\lambda_a(i, \tau) \exp[-S_B - S_J], \\ S_B &= \sum_i \int d\tau [f_{\alpha\alpha}^{\dagger}(i) \partial_{\tau} f_{\alpha}^{\alpha}(i) + i\lambda_a(i) (f_{\alpha\alpha}^{\dagger}(i) f_{\alpha}^{\alpha}(i) - kM)], \\ S_J &= -\frac{J^2}{4NM} \int d\tau d\tau' \left[ \sum_i S_{a\beta}^{\alpha}(i, \tau) S_{b\delta}^{\gamma}(i, \tau') \right] \\ &\quad \times \left[ \sum_j S_{\alpha\alpha}^{\beta}(j, \tau) S_{b\gamma}^{\delta}(j, \tau') \right]. \end{aligned} \quad (2.3)$$

We can now decouple  $S_J$  with a Hubbard-Stratonovich field  $Q_{ab, \beta\delta}^{\alpha\gamma}(\tau, \tau')$  and take the large  $N$  limit. Then the problem reduced to finding saddle points of the single site action

$$\frac{S[Q]}{N} = \frac{J^2}{4M} \int d\tau d\tau' |Q_{ab, \beta\delta}^{\alpha\gamma}(\tau, \tau')|^2 - \ln \mathcal{Z}_f[Q], \quad (2.4)$$

where  $\mathcal{Z}_f[Q]$  is the single site partition function

$$\mathcal{Z}_f[Q] = \int \mathcal{D}f_{\alpha}^{\dagger}(\tau) \mathcal{D}\lambda_a(\tau) \exp[-S_B - S_f], \quad (2.5)$$

$$S_B = \int d\tau [f_{\alpha\alpha}^{\dagger} \partial_{\tau} f_{\alpha}^{\alpha} + i\lambda_a (f_{\alpha\alpha}^{\dagger} f_{\alpha}^{\alpha} - kM)], \quad (2.6)$$

$$\begin{aligned} S_f &= -\frac{J^2}{2M} \int d\tau d\tau' Q_{ab, \beta\delta}^{\alpha\gamma}(\tau, \tau') [f_{\alpha\alpha}^{\dagger}(\tau) f_{\alpha}^{\beta}(\tau) - k\delta_{\beta}^{\alpha}] \\ &\quad \times [f_{b\gamma}^{\dagger}(\tau') f_b^{\delta}(\tau') - k\delta_{\gamma}^{\delta}]. \end{aligned} \quad (2.7)$$

Note that now there is no remaining path integral over  $Q$ . We simply have to find the saddle points of the action  $\mathcal{S}[Q]$  in (2.4).

Let us assume that the saddle point does not break spin rotation symmetry: this is true in both the spin glass, and quantum spin liquid phases. So we make the ansatz [10]

$$Q_{ab, \beta\delta}^{\alpha\gamma}(\tau, \tau') = \delta_{\delta}^{\alpha} \delta_{\beta}^{\gamma} Q_{ab}(\tau - \tau') \quad (2.8)$$

where  $Q_{ab}(\tau)$  is a real function. Also, because there is no path integral over  $Q$ , we can also assume from now on that  $Q_{ab}(\tau)$  is independent of  $\tau$  for  $a \neq b$  [38]. Then (2.4) is replaced by

$$\frac{S[Q]}{N} = \frac{J^2 M}{4} \int d\tau d\tau' [Q_{ab}(\tau - \tau')]^2 - \ln \mathcal{Z}_f[Q] \quad (2.9)$$

while (2.7) is replaced by

$$\begin{aligned} S_f &= -\frac{J^2}{2M} \int d\tau d\tau' Q_{ab}(\tau - \tau') [f_{\alpha\alpha}^{\dagger}(\tau) f_{\alpha}^{\beta}(\tau) f_{b\beta}^{\dagger}(\tau') f_b^{\alpha}(\tau') \\ &\quad - k^2 M]. \end{aligned} \quad (2.10)$$

Finally, we express  $\mathcal{Z}_f[Q]$  as a  $G$ - $\Sigma$  theory [33,39]. We define the spinon Green's function

$$G_{ab}(\tau, \tau') = -\frac{1}{M} \sum_{\alpha} f_{\alpha}^{\alpha}(\tau) f_{b\alpha}^{\dagger}(\tau'). \quad (2.11)$$

Then we can write

$$\begin{aligned} \mathcal{Z}_f[Q] &= \exp \left( -\frac{k^2 J^2}{2} \int d\tau d\tau' \sum_{a,b} Q_{ab}(\tau - \tau') \right) \\ &\quad \times \int \mathcal{D}G_{ab}(\tau, \tau') \mathcal{D}\Sigma_{ab}(\tau, \tau') \mathcal{D}\lambda_a(\tau) \\ &\quad \times \exp[-MI[Q]], \end{aligned} \quad (2.12)$$

where the action  $I[Q]$  is

$$\begin{aligned} I[Q] &= -\ln \det[-\delta'(\tau - \tau') \delta_{ab} - i\lambda_a(\tau) \delta(\tau - \tau') \delta_{ab} \\ &\quad - \Sigma_{ab}(\tau, \tau')] - ik \int d\tau \lambda_a(\tau) \\ &\quad + \int d\tau d\tau' \left[ -\Sigma_{ab}(\tau, \tau') G_{ba}(\tau', \tau) \right. \\ &\quad \left. + \frac{J^2}{2} Q_{ab}(\tau - \tau') G_{ab}(\tau, \tau') G_{ba}(\tau', \tau) \right]. \end{aligned} \quad (2.13)$$

We note that (2.12) and (2.13) constitute an exact formulation of the theory for all  $M$ . Our remaining task is to evaluate the path integral over  $G_{ab}(\tau, \tau')$ ,  $\Sigma_{ab}(\tau, \tau')$ , and  $\lambda_a(\tau)$  in (2.12), and then determine the saddle-point solutions for  $Q_{ab}(\tau)$  in (2.9). The saddle point equations for  $Q$  from (2.9), (2.10), and (2.13) are

$$\begin{aligned} Q_{ab}(\tau - \tau') &= \frac{1}{M^2} \langle f_{\alpha\alpha}^{\dagger}(\tau) f_{\alpha}^{\beta}(\tau) f_{b\beta}^{\dagger}(\tau') f_b^{\alpha}(\tau') \rangle_{\mathcal{Z}_f[Q]} - \frac{k^2}{M} \\ &= -\langle G_{ab}(\tau, \tau') G_{ba}(\tau', \tau) \rangle_{\mathcal{Z}_f[Q]} - \frac{k^2}{M}, \end{aligned} \quad (2.14)$$

but we will find it more convenient to obtain them directly from the functional form of  $S[Q]$ .

From the resulting  $Q_{ab}(\tau)$ , we obtain two different characterizations of the spin glass order [22,23,31,38,40,41]. At

$T = 0$ , we can examine the long-time limit of the replica diagonal  $Q$

$$\bar{q} = \lim_{n \rightarrow 0} \frac{1}{n} \sum_a Q_{aa}(\tau \rightarrow \infty), \quad T = 0, \quad (2.15)$$

and  $\bar{q}$  is one measure of the spin-glass order. Alternatively, we can examine the off-diagonal components, which are necessarily time-independent

$$q_{ab} = Q_{ab}(\tau), \quad a \neq b. \quad (2.16)$$

In the  $n \rightarrow 0$  limit, it is conventional to describe the ultrametric structure of  $q_{ab}$  by the Parisi function  $q(x)$ ,  $0 \leq x \leq 1$ , and the Edwards-Anderson spin glass order parameter is  $q_{EA} = q(1)$ . Consistency between the two different characterizations requires that  $\bar{q} = q_{EA}$ , and this is an important feature of earlier studies of quantum spin glasses [38].

These definitions also allow us to place a bound on spin-glass order. The state with maximum order has the spins frozen in a state in which the fermions occupy the states with, say,  $\alpha = 1, \dots, kM$ , while the other values of  $\alpha$  are empty. Evaluating (2.14) on such a state, we obtain

$$q_{EA} \leq \frac{k(1-k)}{M}. \quad (2.17)$$

Note that (2.17) vanishes as  $M \rightarrow \infty$ , and  $q_{EA}$  is at most  $\mathcal{O}(1/M)$  in the large  $M$  limit; this is consistent with our results in Secs. III and IV. In Appendix A we review the bosonic spinon case of (2.1), and find there that  $q_{EA}$  can be  $\mathcal{O}(M^0)$  in that large  $M$  limit. We also note that for  $SU(2)$ , the definition of the spin glass order from (2.14) is  $q_{EA} = \langle S_i \rangle \cdot \langle S_i \rangle / 2$ , and this is a factor of 2 smaller than the usual definition; so the bound in (2.17) is  $q_{EA} \leq 1/8$ .

We would now like to evaluate  $\ln \mathcal{Z}_f[Q]$  for general  $Q_{ab}(\tau)$ , with  $Q_{ab}$  independent of  $\tau$  for  $a \neq b$ . We first do this at  $M = \infty$  in Sec. III, and then examine  $1/M$  corrections in Sec. IV.

### III. LARGE $M$ LIMIT

Assuming a general  $Q_{ab}(\tau)$ , the large  $M$  limit of the path-integral in (2.12) leads to the following saddle-point equations for the fermion Green's function and self-energy

$$\begin{aligned} \Sigma_{ab}(\tau) &= J^2 Q_{ab}(\tau) G_{ab}(\tau), \\ G_{ab}(i\omega) &= [i\omega \delta_{ab} - \Sigma_{ab}(i\omega)]^{-1}, \end{aligned} \quad (3.1)$$

where  $\lambda_a = 0$  at the  $k = 1/2$  saddle-point because of particle-hole symmetry. However, we must keep in mind that there cannot be any off-diagonal components of the fermion Green's function at the saddle-point, because it is not possible for fermions to condense. So we write

$$G_{ab}(\tau, \tau') = G_Q(\tau - \tau') \delta_{ab}, \quad M = \infty, \quad (3.2)$$

and similarly for  $\Sigma_{ab}$ . From the large  $N$  saddle-point equation for  $Q_{ab}$  in (2.14), we see that  $Q_{ab}$  must also be replica diagonal,

$$Q_{ab}(\tau) = Q(\tau) \delta_{ab}, \quad M = \infty, \quad (3.3)$$

and so there is no spin glass order at  $M = \infty$  [10]. The large  $M$  saddle point equations (3.1) therefore reduce to

$$\begin{aligned} \Sigma_Q(\tau) &= J^2 Q(\tau) G_Q(\tau), \\ G_Q(i\omega) &= [i\omega - \Sigma_Q(i\omega)]^{-1}. \end{aligned} \quad (3.4)$$

These equations hold for general  $Q(\tau)$ , and we have emphasized this by the subscript  $Q$  on  $G$  and  $\Sigma$ . Upon including the large  $N$  saddle point equation for  $Q$  in (2.14), we obtain

$$Q(\tau) = -G_Q(\tau) G_Q(-\tau), \quad M = \infty. \quad (3.5)$$

The combination of (3.4) and (3.5) yields precisely the large  $N$  equations of the fermion of the complex SYK model [10]. In the following sections, we include corrections from the replica off-diagonal and two-time fluctuations of  $G_{ab}(\tau, \tau')$  and  $\Sigma_{ab}(\tau, \tau')$ , and these will modify (3.5), but we will continue to use (3.4).

For completeness, we also present the expressions for the path integral in (2.13):

$$\begin{aligned} -\frac{\ln \mathcal{Z}_f[Q]}{Mn} &= \frac{I[Q]}{n} + \frac{k^2 J^2}{2Mn} \int d\tau d\tau' \sum_{a,b} Q_{ab}(\tau - \tau'), \\ \frac{I[Q]}{n} &= -\ln \det[-\delta'(\tau - \tau') - \Sigma_Q(\tau - \tau')] \\ &\quad + \int d\tau d\tau' \left[ -\Sigma_Q(\tau - \tau') G_Q(\tau' - \tau) \right. \\ &\quad \left. + \frac{J^2}{2} Q(\tau - \tau') G_Q(\tau - \tau') G_Q(\tau' - \tau) \right]. \end{aligned} \quad (3.6)$$

### IV. $1/M$ EXPANSION

This section will describe  $1/M$  corrections to  $\ln \mathcal{Z}_f[Q]$  in (2.9). We will see below that these corrections are characterized by a divergent spin glass susceptibility, and so spin glass order is present for any finite  $M$  [23].

To evaluate these finite  $M$  fluctuations, we extend (3.2) for the fermion Green's function and self-energy, and for the constraint Lagrange multiplier by

$$\begin{aligned} G_{ab}(\tau, \tau') &= G_Q(\tau - \tau') \delta_{ab} + \delta G_{ab}(\tau, \tau'), \\ \Sigma_{ab}(\tau, \tau') &= \Sigma_Q(\tau - \tau') \delta_{ab} + \delta \Sigma_{ab}(\tau, \tau') \\ &\quad - i\delta \lambda_a(\tau) \delta(\tau - \tau') \delta_{ab}, \\ \lambda_a(\tau) &= \bar{\lambda}_a + \delta \lambda_a(\tau), \end{aligned} \quad (4.1)$$

where  $\bar{\lambda}_a = 0$  at the  $M = \infty$  saddle point for the particle-hole symmetric case  $k = 1/2$ . We can use the gauge invariance discussed in Appendix B to choose a gauge in which  $\delta \lambda_a(\tau)$  is  $\tau$  independent. Then the time-independent value of  $\delta \lambda_a$  can be absorbed into  $\bar{\lambda}_a$ , and evaluating the path integral over  $\delta \lambda_a(\tau)$  to relative order  $1/M^2$  reduces to computing the shift in the saddle-point value of  $\bar{\lambda}_a$  to order  $1/M$  [42,43]. This shift in the value of  $\bar{\lambda}_a$  has to be included in  $G_Q$ . Also, while the expectation values of  $G_{ab}(\tau, \tau')$ ,  $\Sigma_{ab}(\tau, \tau')$  must depend only upon  $\tau - \tau'$  and have to be replica diagonal, the fluctuations  $\delta G_{ab}(\tau, \tau')$ ,  $\delta \Sigma_{ab}(\tau, \tau')$  of both replica diagonal and replica off-diagonal components must include full dependence on both  $\tau$  and  $\tau'$ .

$$K_{ab;cd}(\tau_1, \tau_2; \tau_3, \tau_4) = \begin{array}{c} (a, \tau_1) \quad G_Q \quad (c, \tau_3) \\ \left. \begin{array}{c} \text{---} \\ \text{---} \\ \text{---} \\ \text{---} \end{array} \right\} Q_{ab} \\ (b, \tau_2) \quad G_Q \quad (d, \tau_4) \end{array}$$

FIG. 2. Pictorial representation of the ‘‘ladder’’ kernel featuring in the fluctuation determinant.

### A. Determinant of quadratic fluctuations

We begin with the first  $1/M$  corrections, which are associated with quadratic fluctuations of  $\delta G_{ab}(\tau, \tau')$ ,  $\delta \Sigma_{ab}(\tau, \tau')$ . Expanding the action (2.13) to second order in fluctuations around the large  $M$  saddle point, we find the quadratic action

$$\begin{aligned} I_{(2)}[Q] &= \frac{1}{2} \int d\tau_1 \cdots d\tau_4 \sum_{a,b,c,d} \delta X_{ab}^T(\tau_1, \tau_2) \\ &\quad \times \cdot A_{ab;cd}(\tau_1, \tau_2; \tau_3, \tau_4) \cdot \delta X_{cd}(\tau_3, \tau_4) \\ &\equiv \frac{1}{2} \delta \mathbf{X}^T \cdot \mathbf{A} \cdot \delta \mathbf{X}, \end{aligned} \quad (4.2)$$

where matrix multiplication involves the following structures:

$$\begin{aligned} \delta \mathbf{X} &\equiv \delta X_{ab}(\tau_1, \tau_2) \equiv \begin{pmatrix} \delta G_{ab}(\tau_1, \tau_2), \\ \delta \Sigma_{ab}(\tau_1, \tau_2) \end{pmatrix}, \\ \mathbf{A} &\equiv A_{ab;cd}(\tau_1, \tau_2; \tau_3, \tau_4) \\ &\equiv \begin{pmatrix} J^2 Q_{ab}(\tau_1, \tau_2) \delta(\tau_{14}) \delta(\tau_{32}) & -\delta(\tau_{14}) \delta(\tau_{32}) \\ -\delta(\tau_{14}) \delta(\tau_{32}) & G_Q(\tau_{14}) G_Q(\tau_{32}) \end{pmatrix} \delta_{ad} \delta_{bc}, \end{aligned} \quad (4.3)$$

and the dot product is defined as indicated in terms of integration over pairs of time arguments and summation over pairs of replica indices.

Having reduced the problem to a Gaussian integral, we are now in a position to evaluate the contribution to the free energy  $\mathcal{F} = -(M\beta n)^{-1} \ln \mathcal{Z}_f[Q]$  originating from quadratic fluctuation determinants. We denote this contribution as

$$\begin{aligned} \beta n \mathcal{F}_{sg} &= \frac{k^2 J^2}{2} \int d\tau d\tau' \sum_{a,b} Q_{ab}(\tau, \tau') \\ &\quad + \frac{1}{2} \ln \det \mathbf{A} + \mathcal{O}(M^{-1}). \end{aligned} \quad (4.4)$$

Let us focus on the fluctuation determinant of  $\mathbf{A}$ , which can be expanded in terms of a ladder kernel:

$$\begin{aligned} \frac{1}{2} \ln \det \mathbf{A} &= \frac{1}{2} \text{Tr} \ln(\mathbf{K} - \mathbf{1}) \\ &= -\frac{1}{2} \text{Tr} \mathbf{K} - \frac{1}{4} \text{Tr} \mathbf{K}^2 \\ &\quad - \frac{1}{6} \text{Tr} \mathbf{K}^3 + \dots, \end{aligned} \quad (4.5)$$

where the ladder kernel and the identity operator are defined as

$$\begin{aligned} \mathbf{K} &\equiv K_{ab;cd}(\tau_1, \tau_2; \tau_3, \tau_4) \\ &\equiv J^2 Q_{ab}(\tau_1, \tau_2) G_Q(\tau_1 - \tau_3) G_Q(\tau_4 - \tau_2) \delta_{ac} \delta_{bd}, \\ \mathbf{1} &\equiv \delta(\tau_1 - \tau_3) \delta(\tau_4 - \tau_2) \delta_{ac} \delta_{bd}. \end{aligned} \quad (4.6)$$

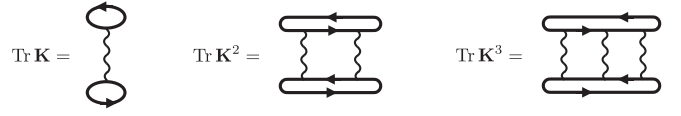


FIG. 3. Some diagrams contributing to  $-\ln \mathcal{Z}_f[Q]$  at the first subleading order, i.e.,  $\mathcal{O}(M^0)$ .

In Fig. 2, we introduce a diagrammatic notation for the kernel.<sup>1</sup> Figure 3 further illustrates the above contributions to the free energy diagrammatically. One can check that the first diagram,  $\text{Tr} \mathbf{K}$ , is canceled by the first term in (4.4).<sup>2</sup> The traces of higher powers of the ladder kernel yield:

$$\begin{aligned} -\frac{1}{4} \text{Tr} \mathbf{K}^2 &= -\frac{J^4}{4} \int d\tau_1 \cdots d\tau_4 \\ &\quad \times \sum_{a,b} Q_{ab}(\tau_1, \tau_2) Q_{ab}(\tau_3, \tau_4) R_Q^{(2)}(\tau_{13}) R_Q^{(2)}(\tau_{24}), \\ -\frac{1}{6} \text{Tr} \mathbf{K}^3 &= \frac{J^6}{6} \int d\tau_1 \cdots d\tau_6 \\ &\quad \times \sum_{a,b} Q_{ab}(\tau_1, \tau_2) Q_{ab} \\ &\quad \times (\tau_3, \tau_4) Q_{ab}(\tau_5, \tau_6) R_Q^{(3)}(\tau_{13}, \tau_{35}) R_Q^{(3)}(\tau_{24}, \tau_{46}), \end{aligned} \quad (4.8)$$

and so on, where the time splitting functions are given by the spinon loops

$$R_Q^{(2)}(\tau) \equiv G_Q(\tau) G_Q(-\tau),$$

$$R_Q^{(3)}(\tau, \tau') \equiv G_Q(\tau) G_Q(\tau') G_Q(-\tau - \tau'), \quad \dots \quad (4.9)$$

Consider now the ansatz for  $Q_{ab}$ , which we described in (2.15) and (2.16). Without loss of generality, we parametrize this ansatz as follows:

$$Q_{ab}(\tau, \tau') = [Q(\tau - \tau') + \bar{q}] \delta_{ab} + q_{ab}, \quad q_{aa} = 0. \quad (4.10)$$

We then find a simple expression for the contribution of  $\mathcal{Z}_f[Q]$  to the free energy per spin. In particular, the subleading terms described above yield a contribution to the free energy, which we denote as

$$\begin{aligned} \mathcal{F}_{sg} &\equiv -\frac{\ln \mathcal{Z}_f[Q]}{\beta n} \\ &= -c_0 - c_1 \bar{q} - c_2 \bar{q}^2 - d_2 \beta \left( \bar{q}^2 + \frac{1}{n} \sum_{a \neq b} q_{ab}^2 \right) \\ &\quad - c_3 \bar{q}^3 - c_4 \bar{q}^4 - d_4 \beta \left( \bar{q}^4 + \frac{1}{n} \sum_{a \neq b} q_{ab}^4 \right) + \dots, \end{aligned} \quad (4.11)$$

<sup>1</sup>The diagrams focus on the structure of replica indices. To recover the fermionic description one uses a double line notation where the wiggly line fattens into two lines carrying  $SU(M)$  indices.

<sup>2</sup>In the computation of  $\text{Tr} \mathbf{K}$ , we use the following point splitting prescription to be consistent with the fermionic description:

$$\text{Tr} \mathbf{K} = \lim_{\varepsilon \rightarrow 0} \int d\tau_1 d\tau_2 \sum_{a,b} \mathbf{K}_{ab;ab}(\tau_1, \tau_2; \tau_1 + \varepsilon, \tau_2 - \varepsilon). \quad (4.7)$$

where we organize the expression as an expansion in powers of  $\bar{q}$  and  $q_{ab}$ . The coefficients are given by

$$d_2 = \frac{J^4}{4} R_Q^{(2)}(i\omega = 0)^2, \quad d_4 = \frac{J^8}{8} R_Q^{(4)}(i\omega_1 = 0, i\omega_2 = 0, i\omega_3 = 0)^2, \dots, \quad (4.12)$$

and

$$\begin{aligned} c_0 &= \frac{J^4}{4\beta} \sum_{\omega} R_Q^{(2)}(i\omega)^2 Q(i\omega)^2 + \frac{J^6}{6\beta^2} \sum_{\omega, \omega'} R_Q^{(3)}(i\omega, i\omega')^2 Q(i\omega) Q(i\omega - i\omega') Q(i\omega') \\ &\quad + \frac{J^8}{8\beta^3} \sum_{\omega, \omega', \omega''} R_Q^{(4)}(i\omega, i\omega', i\omega'')^2 Q(i\omega) Q(i\omega - i\omega') Q(i\omega' - i\omega'') Q(i\omega'') + \dots, \\ c_1 &= \frac{J^4}{2} R_Q^{(2)}(0)^2 Q(0) + \frac{J^6}{2\beta} \sum_{\omega} R_Q^{(3)}(i\omega, 0)^2 Q(i\omega)^2 + \frac{J^8}{2\beta^2} \sum_{\omega, \omega'} R_Q^{(4)}(i\omega, i\omega', 0)^2 Q(i\omega) Q(i\omega - i\omega') Q(i\omega') + \dots, \\ c_2 &= \frac{J^8}{4\beta} \sum_{\omega} [2R_Q^{(4)}(i\omega, 0, 0)^2 + R_Q^{(4)}(i\omega, i\omega, 0)^2] Q(i\omega)^2 + \dots, \\ c_3 &= \frac{J^8}{2} R_Q^{(4)}(0, 0, 0)^2 Q(0) + \dots, \end{aligned} \quad (4.13)$$

where all  $Q$  and  $R_Q^{(n)}$  in the above equations are frequency space expressions. We also used their symmetry properties,

$$R_Q^{(n)}(-i\omega_1, \dots, -i\omega_{n-1}) = (-1)^n R_Q^{(n)}(i\omega_1, \dots, i\omega_{n-1}), \quad (4.14)$$

to simplify some expressions and to conclude that coefficients such as  $d_3 = d_5 = \dots = 0$  (for the particle-hole symmetric case  $k = 1/2$ ). Note that we have reinstated explicit  $\beta$  dependence in the above formulas in order to make manifest that only the terms multiplying  $d_k$  are linearly proportional to  $\beta$  in the low temperature limit,  $\beta \rightarrow \infty$ . In general, we find that the coefficients of these linearly divergent terms are always negative and given by

$$d_{2k} = \frac{J^{4k}}{4k} \left( \frac{1}{\beta} \sum_{\omega} G_Q(i\omega)^{2k} \right)^2 \quad (k = 1, 2, \dots). \quad (4.15)$$

When evaluated on the spin liquid Green's function  $G_Q(i\omega) \sim 1/\sqrt{\omega}$ , we find a further divergence in the values of  $d_{2k}$  in (4.15):  $d_{2k} \sim \beta^{2k-2}$ . However, this divergence is cutoff when we compute  $d_{2k}$  using the self-consistent results for  $G_Q(i\omega)$  to be computed in Section V: the cutoff frequency scale is  $\omega_*$  in (1.5), and hence  $d_{2k} \sim q_{EA}^{2-2k}$ . The net contribution of all the  $d_{2k}$  terms in (4.11) to the free energy is therefore of order  $\beta q_{EA}^2$ . For  $k = 1$ , there is an additional logarithm of  $\beta$  (or  $\omega_*$ ), as noted below in (4.18).

Higher orders in the  $1/M$  expansion can be computed in a similar fashion. In short, these are characterized by more complicated diagrams build from the kernel  $\mathbf{K}$ . We elaborate on this in Appendix C.

## B. Free energy

In order for the theory to be consistent, we will need to ensure that physical quantities such as the free energy are finite as  $\beta \rightarrow \infty$ . As we discuss next, this follows indeed from the equations of motion for the spin glass parameters  $\bar{q}$  and  $q_{ab}$ .

The free energy including the corrections to first subleading in the  $1/M$  expansion reads as follows:

$$\begin{aligned} \beta n \mathcal{F} &\equiv \frac{S[Q]}{NM} = \frac{\beta n J^2}{4} \left[ \frac{1}{\beta} \sum_{\omega} Q(i\omega)^2 + 2\bar{q} Q(i\omega = 0) \right. \\ &\quad \left. + \beta \left( \bar{q}^2 + \frac{1}{n} \sum_{a \neq b} q_{ab}^2 \right) \right] + I[Q] \\ &\quad + \frac{\beta n}{M} \mathcal{F}_{sg} + \mathcal{O}(M^{-2}), \end{aligned} \quad (4.16)$$

where the leading terms were given in (2.9) and (3.6), while the  $\mathcal{F}_{sg}$  term was computed in (4.11). Of particular importance is the term quadratic in the spin glass order parameter

$$\frac{S[Q]}{NM} = \frac{\beta^2 n J^2}{4} \left( \bar{q}^2 + \frac{1}{n} \sum_{a \neq b} q_{ab}^2 \right) \left[ 1 - \frac{J^2}{M} \chi_{\text{loc}}^2 \right] + \dots, \quad (4.17)$$

where  $\chi_{\text{loc}} = -R_Q^{(2)}(i\omega = 0)$  is the local spin susceptibility. The term in square brackets in (4.17) is precisely that appearing in the denominator of the spin glass susceptibility [23]. In the SYK spin liquid state [10] [this is evident from the Hilbert transform of (1.3)],

$$\chi_{\text{loc}} = \int_0^{\beta} Q(\tau) d\tau = \frac{1}{J\sqrt{\pi}} \ln(\beta J), \quad (4.18)$$

and so the term in square brackets becomes negative at low enough temperatures provided  $M$  is finite. Once this term is negative, spin glass order will appear, and we obtain an estimate

$$T_c \sim J \exp(-\sqrt{M\pi}) \quad (4.19)$$

for the critical temperature [23]. For temperatures below  $T_c$ ,  $\chi_{\text{loc}}$  is finite at  $T = 0$  in the presence of spin glass order, as we will see in Sec. V.

The simplest ansatz for evaluating the free energy assumes a replica symmetric off-diagonal spin glass order of the form

$q_{a \neq b} = q_{EA}$ . In this case, we employ the following simplification as  $n \rightarrow 0$ :

$$\frac{1}{n} \sum_{a \neq b} q_{ab}^{\ell} = (n-1)q_{EA}^{\ell} \longrightarrow -q_{EA}^{\ell}. \quad (4.20)$$

Extremization of  $\mathcal{F}$  with respect to  $q_{EA}$  then yields the following equation of motion:

$$\frac{J^2}{2} q_{EA} = \frac{1}{M} [2d_2 q_{EA} + 4d_4 q_{EA}^3 + \dots] + \mathcal{O}(M^{-2}). \quad (4.21)$$

Similarly, extremization with respect to  $\bar{q}$  gives

$$\begin{aligned} & \frac{J^2}{2} \left[ \bar{q} + \frac{1}{\beta} Q(0) \right] \\ &= \frac{1}{M} \left[ 2d_2 \bar{q} + 4d_4 \bar{q}^3 + \dots \right. \\ & \quad \left. + \frac{1}{\beta} (c_1 + 2c_2 \bar{q} + 3c_3 \bar{q}^2 + 4c_4 \bar{q}^3 + \dots) \right] + \mathcal{O}(M^{-2}). \end{aligned} \quad (4.22)$$

Evidently, these equations imply

$$\bar{q} = q_{EA} + \mathcal{O}(\beta^{-1}). \quad (4.23)$$

Evaluated on this solution, the free energy is indeed finite as  $\beta \rightarrow \infty$  since all dangerous terms are of the following form as  $n \rightarrow 0$ :

$$\begin{aligned} \mathcal{F} &= \beta \left\{ \frac{J^2}{4} (\bar{q}^2 - q_{EA}^2) - \frac{1}{M} \sum_{k \geq 1} d_{2k} (\bar{q}^{2k} - q_{EA}^{2k}) + \mathcal{O}(M^{-2}) \right\} \\ &+ \mathcal{O}(\beta^0) = \mathcal{O}(\beta^0), \end{aligned} \quad (4.24)$$

where in the last step we used the relation (4.23). In Appendix C, we compute some examples of contributions at higher orders in the  $1/M$  expansion, and show that these also have a finite limit as  $\beta \rightarrow \infty$ .

A notable feature of this analysis is that the free energy is finite in the  $\beta \rightarrow \infty$  limit, even though there are many individual terms that diverge in this limit. There is a delicate cancellation of the divergent terms between the replica diagonal and off-diagonal contributions in the  $n \rightarrow 0$  limit [38]. This cancellation was overlooked in an early work on the random quantum magnet [44]: they only included the replica diagonal terms, which in fact diverge as  $\beta \rightarrow \infty$ , and so their energy estimates are not meaningful. Such divergent contributions to the free energy are also present in various EDMFT theories of strongly correlated phases [45–50], and we believe that the energy estimates in such theories are not reliable in the phase with long-range order at very low temperatures.

## V. SPECTRUM OF THE SPIN GLASS STATE

We have seen in Sec. IV that the order parameter characterizing the spin glass ground state,  $q_{ab}$ , is determined entirely by corrections to the leading large  $M$  saddle point. Moreover, as  $\beta \rightarrow \infty$ , the long time limit of the spin autocorrelation function,  $\bar{q}$ , equals the Edwards-Anderson order parameter  $q_{EA}$  (which is in turn determined from  $q_{ab}$ ). In this section,

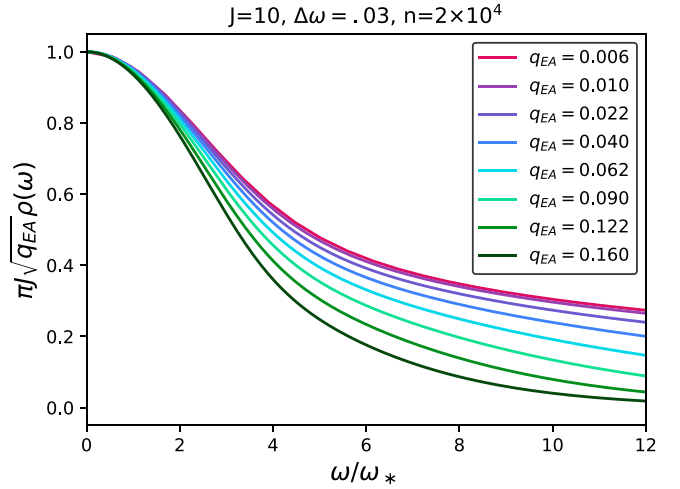


FIG. 4. Numerical results for the spinon spectral density obtained by the solution of (3.4) and (5.1). The results scale as in (5.2) for small  $q_{EA}$ . The solutions were obtained with  $n$  frequency points.

we will address the feedback of the onset of spin glass order on the spinon Green's function and the dynamic spin susceptibility.

In Sec. III, we determined the large  $M$  equations, (3.4), obeyed by the fermion Green's function for a general spin autocorrelation function  $Q(\tau)$ . In the spin glass phase, we mapped  $Q(\tau) \rightarrow Q(\tau) + \bar{q}$  in (4.10) to allow for a nonzero long time limit. The computations of Section IV, will lead to corrections to  $Q(\tau)$  at order  $1/M$ , along with allowing for a nonzero  $\bar{q}$ . In our analysis here, we will ignore the  $1/M$  corrections to  $Q(\tau)$ , as they have a structure similar to that obtained in the  $M = \infty$  theory. However, we will keep the nonzero value of  $\bar{q} = q_{EA}$  because it has a singular effect on the low frequency fermion spectrum, as we will now show.

The upshot of this discussion is that we can determine the fermion Green's function by solving (3.4), while (3.5) is

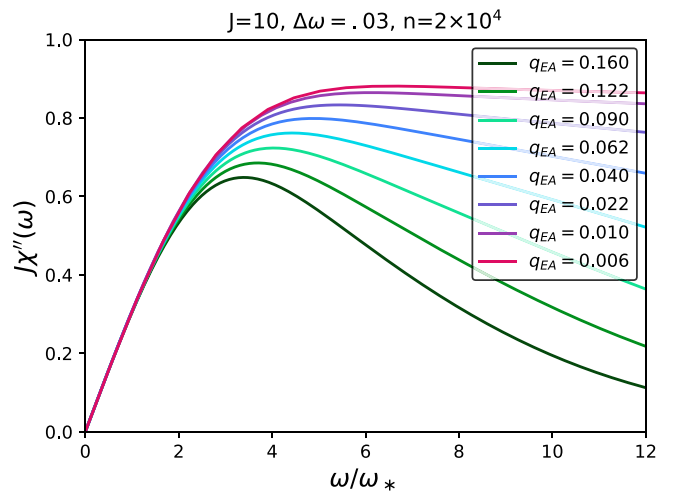


FIG. 5. Numerical results for the spin spectral density obtained by the solution of (3.4) and (5.1). The results scale as in (5.3) for small  $q_{EA}$ .

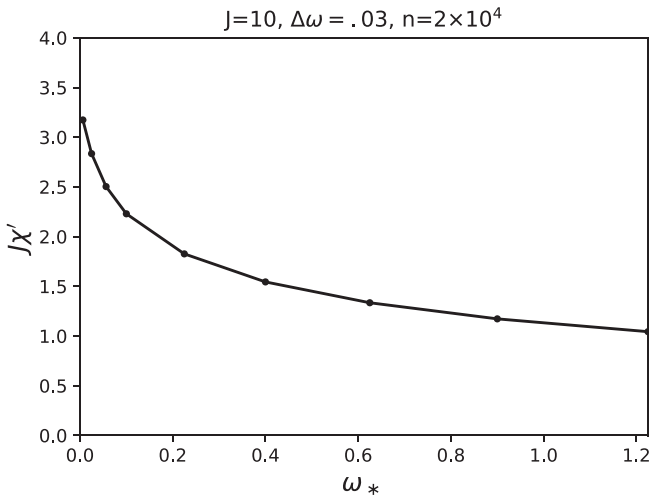


FIG. 6. The real part of the local susceptibility  $\chi' = \chi_{\text{loc}}$ .

modified to

$$Q(\tau) = -G_Q(\tau)G_Q(-\tau) + q_{EA}. \quad (5.1)$$

Remarkably, the equations (3.4) and (5.1) have been solved previously [51,52], in different contexts. Reference [51] considered a random  $t$ - $J$  model in a particular large  $M$  limit, with r.m.s. exchange  $J$ , and r.m.s. hopping  $t$ . Ref. [52] considered a SYK model with a random four-fermion interaction term with r.m.s. strength  $J$ , and a random two-fermion hopping term  $t$ . The equations of the latter model map onto (3.4) and (5.1) with  $t = J\sqrt{q_{EA}}$ . Their main result was that there was a crossover from SYK non-Fermi liquid behavior to Fermi liquid behavior at a coherence energy scale  $\sim t^2/J$  [51,52] which equals  $Jq_{EA}$ . From this, we can obtain the structure of the low frequency spectrum in the spin glass phase when  $q_{EA} \ll 1$ . For the spinon spectral density, we have

$$\rho(\omega) = -\frac{1}{\pi} \text{Im} G_Q(\omega) = \frac{1}{\pi \sqrt{J\omega_*}} \Phi_\rho(\omega/\omega_*), \quad (5.2)$$

with  $\omega_*$  given by (1.5). The scaling function  $\Phi_\rho$  obeys  $\Phi_\rho(0) = 1$ , and  $\Phi_\rho(\bar{\omega} \gg 1) \sim 1/\sqrt{\bar{\omega}}$ . We present result for  $\rho(\omega)$  in Fig. 4, comparing with the scaling in (5.2).

Similarly, for the spin spectral density we have

$$\chi''(\omega) = -\text{Im} Q(\omega) = \frac{1}{J} \Phi_\chi(\omega/\omega_*). \quad (5.3)$$

Note that the full dynamic spin susceptibility has the delta function in (1.4), which is not included in (5.3). The scaling function  $\Phi_\chi(\bar{\omega})$  has the form given by (1.6) at  $\bar{\omega} \ll 1$ , and by (1.3) for  $\bar{\omega} \gg 1$ , and this is illustrated in Fig. 5.

The real part of the local spin response function, i.e., the local static susceptibility has a logarithmic contribution which violates scaling: the  $q_{EA} = 0$  result in (4.18) is replaced by

$$\chi_{\text{loc}} = \frac{1}{J\sqrt{\pi}} \ln(J/\omega_*), \quad T = 0. \quad (5.4)$$

This is illustrated in Fig. 6.

With these results for  $G_Q$ , the entropy can be computed from the expression for the free energy in (3.6). We expect

results similar to those in Ref. [52], with an entropy that vanishes linearly in temperature, with a co-efficient that is enhanced as  $1/\omega_*$ . This was anticipated in Fig. 1. We note that the bosonic spinon approach also yielded numerical results consistent with a linear-in- $T$  entropy [23], and a linear-in- $T$  entropy has also been found in other solvable quantum spin glass models [31].

## VI. COMPLEXITY

In the quantum spin liquid phase, the model features an exponential density of states and an extensive (in  $N$ ) thermodynamic entropy. As the system enters the spin glass phase and thermal fluctuations are further reduced, the thermodynamic entropy approaches zero. Instead, an extensive configurational entropy counts an exponential number of possible meta-stable glass states. This configurational entropy is often referred to as the complexity  $\Sigma$ , which can be expressed as a functional of the free energy  $\mathcal{F}$  and the break-point parameter  $m$  of the replica symmetry breaking ansatz [26–28].<sup>3</sup> The number of meta-stable states in a given free energy band of width  $1/(m\beta)$  is then given by

$$\Omega(\mathcal{F}, m) = e^{N\Sigma(\mathcal{F}, m)}. \quad (6.1)$$

In practice we compute the complexity as the Legendre transform of the free energy with respect to  $m$ . As a function of  $(\beta, m)$ , this can be computed as

$$\Sigma(\beta, m) = \beta m^2 \partial_m \mathcal{F}(\beta, m). \quad (6.2)$$

We will now show how to evaluate this expression in our model.

Consider the following simple Landau free energy, which exhibits the basic structure of our model:

$$\begin{aligned} \mathcal{F}_{\text{sg}}[\bar{q}, q_{ab}] = & -d_2\beta \left( \bar{q}^2 + \frac{\text{Tr}q^2}{n} \right) \\ & - \frac{e_3}{3} \beta^2 \left( \bar{q}^3 + 3\bar{q} \frac{\text{Tr}q^2}{n} + \frac{\text{Tr}q^3}{n} \right) \\ & - d_4\beta \left( \bar{q}^4 + \frac{1}{n} \sum_{a,b} q_{ab}^4 \right) + \dots \end{aligned} \quad (6.3)$$

The coefficients  $d_2, e_3, d_4$  are dimensionful but finite as  $\beta \rightarrow \infty$ . We computed  $d_2$  and  $d_4$  in Sec. IV; the coefficient  $e_3$  is generated at  $\mathcal{O}(M^{-1})$ , see Appendix C. We dropped terms that do not contribute to the zero-temperature complexity, as well as terms at higher orders in  $\bar{q}$  and  $q_{ab}$ .

To evaluate the free energy, we now go beyond the replica symmetric ansatz and consider full replica symmetry breaking (FRSB). This is implemented by starting from the Parisi ansatz for  $k$ -step replica symmetry breaking [53] and then

<sup>3</sup>See also Ref. [29] for a review, Ref. [30] for a textbook discussion, and Ref. [31] for a recent application.



considering the limit  $k \rightarrow \infty$ : we first make an ansatz for  $q_{ab}$  with constant blocks along the diagonal and then succes-

sively refine the structure by breaking up blocks into smaller blocks:

$$q_{ab} = \begin{pmatrix} \boxed{A_{m_1}} & & & & \\ & \boxed{A_{m_1}} & & & \\ & & q_0 & & \\ & & & \ddots & \\ & q_0 & & & \boxed{A_{m_1}} \\ & & & & & \boxed{A_{m_1}} \end{pmatrix}, \quad A_{m_1} = \begin{pmatrix} \boxed{A_{m_2}} & & & & \\ & \boxed{A_{m_2}} & & & \\ & & q_1 & & \\ & & & \ddots & \\ q_1 & & & & \boxed{A_{m_2}} \\ & & & & & \boxed{A_{m_2}} \end{pmatrix} \quad (6.4)$$

and so on, where  $A_{m_i}$  is an  $m_i \times m_i$  matrix with blocks  $A_{m_{i+1}}$  along the diagonal and all off-diagonal entries filled with  $q_i$  such that  $n = \sum_i m_i$ . In the analytic continuation  $n \rightarrow 0$  we replace the matrix  $q_{ab}$  by a monotonously increasing function  $q(x)$ , which extrapolates the structure above. The variable  $x \in [0, 1]$  parametrizes continuous breaking of replica symmetry. The analog of the Edwards-Anderson parameter is  $q_{EA} = q(x = 1)$ .

With this ansatz, the free energy (6.3) then becomes a functional of  $q(x)$ :

$$\mathcal{F}_{sg}[\bar{q}, q(x)] = \int_0^1 dx \left\{ d_2 \beta (q(x)^2 - \bar{q}^2) + d_4 \beta (q(x)^4 - \bar{q}^4) - \frac{e_3}{3} \beta^2 \left( \bar{q}^3 - 3\bar{q} q(x)^2 + x q(x)^3 + 3q(x) \times \int_0^x dy q(y)^2 \right) + \dots \right\} \quad (6.5)$$

Extremizing the action with respect to  $q(x)$  leads to the following continuous solution [54]:

$$q(x) = \begin{cases} \frac{x}{m} q_{EA}, & x \in [0, m] \\ q_{EA}, & x \in [m, 1] \end{cases}, \quad (6.6)$$

where  $m \equiv \frac{12d_4}{e_3\beta} q_{EA}$  plays the role of the break point parameter of an equilibrium solution. The extremization procedure also relates the value of the diagonal contribution  $\bar{q}$  to  $q_{EA}$ :

$$\bar{q} = q_{EA} - \frac{d_2 + 6d_4 q_{EA}^2}{e_3 \beta}. \quad (6.7)$$

Note that we do not separately extremize with respect to  $\bar{q}$  because even perturbatively the ansatz (6.3) only captures part of the full  $\bar{q}$  dependence of our system.

Evaluated on the saddle point solution for  $q(x)$ , the free energy takes the following value:

$$\mathcal{F}_{sg}(m, \beta_e) = -\frac{d_2^4 d_4 m^3}{e_3^4 \beta_e^3} - \frac{d_2^3 m(4 - 2m + m^2)}{6e_3^2 \beta_e} + \frac{d_2^2 (2 - m)(4 - 2m + m^2) \beta_e}{96d_4} + \frac{d_2 e_3^2 (2 - m)^3 \beta_e^3}{6(24d_4)^2} + \frac{e_3^4 [48 - 5m(4 - m)^2] \beta_e^5}{15(48d_4)^3} + \dots, \quad (6.8)$$

where  $\beta_e \equiv m\beta$  is an effective temperature, conjugate to the free energy. Expanding in large  $\beta$ , we obtain

$$\mathcal{F}_{sg}(m, \beta) = \frac{d_2^2}{e_3} q_{EA}^2 + \frac{4d_2 d_4}{e_3} q_{EA}^3 + \frac{36d_4^2}{5e_3} q_{EA}^5 + \mathcal{O}(\beta^{-1}) + \dots \quad (6.9)$$

Note again that the free energy is finite as  $\beta \rightarrow \infty$ . This was not guaranteed to happen. It is a consequence of the specific way in which  $\bar{q}$  appeared in (6.3) and of the extremization condition (6.7).

In order to compute the low temperature complexity, we take an  $m$  derivative (at fixed  $\beta$ ) and then expand in large  $\beta$ . According to (6.2), we find

$$\Sigma(m, \beta) \equiv \beta m^2 \partial_m \mathcal{F}_{sg}(m, \beta) \equiv \beta_e^2 \partial_{\beta_e} \mathcal{F}_{sg}(m, \beta_e) = \frac{12d_4}{e_3^2} q_{EA}^2 (d_2 + 6d_4 q_{EA}^2 + \dots)^2 + \mathcal{O}(\beta^{-1}). \quad (6.10)$$

The fact that the complexity  $\Sigma$  is finite as  $\beta \rightarrow \infty$  means that the spin glass at zero temperature is characterized by an extensive number  $e^{N\Sigma}$  of metastable states.

## VII. DISCUSSION

The initial analysis [10] of the  $SU(M)$  random quantum magnet (2.1) found a gapless quantum spin liquid ground state in the large  $M$  limits realized by fermionic and bosonic spinons, and both limits yielded a ‘‘marginal’’ dynamic spin susceptibility with  $\chi''(\omega) \sim \text{sgn}(\omega)$  at small  $\omega$ . This fractionalized spin liquid is unstable to spin glass order at low enough temperatures for any finite  $M$  [23], and (4.19) contains an estimate of the critical temperature for fermionic spinons. A theory of a spin glass ground state was presented in Refs. [22,23] using bosonic spinons, in which case the spin glass order can be large, with  $q_{EA} = \mathcal{O}(M^0)$  (see (A2)). However, numerical studies of the  $SU(2)$  case show that the spin glass order is small [16,17], and the intermediate frequency spin spectrum was a better match with the large  $M$  theory with fermionic spinons [14,17]. Here we have presented an analysis which is closest to the numerical observations: a theory for the onset of weak spin glass order using fermionic spinons, where  $q_{EA}$  is at most  $\mathcal{O}(M^{-1})$  [see (2.17)]. We identified a frequency scale  $\omega_* = J q_{EA}$ , and showed that  $\chi''(\omega) \sim \omega$  in

the fermionic spinon theory, as had also been found for small  $\omega$  in the bosonic spinon theory. For the case of small  $q_{EA}$ , there is a universal crossover from the physics of a quantum spin liquid with fractionalized spinons for  $\omega > \omega_*$ , to the physics of a confining spin glass for  $\omega < \omega_*$ , and we obtained results for the crossover functions.

In Sec. V, we mapped the crossover from the spectrum of the SYK spin liquid to the spin glass to the crossover from non-Fermi liquid to Fermi liquid behavior in the model of Ref. [52]. We now comment on why this can be interpreted as a crossover from fractionalization to confinement in our context of the random quantum magnet. Unlike the case for the model of Ref. [52], the fermions in our quantum magnet, and in the  $t$ - $J$  models of Refs. [51,55], carry a U(1) gauge charge: (2.2) is invariant under the gauge transformation  $f^\alpha(i) \rightarrow f^\alpha(i)e^{i\phi_i(\tau)}$  (see Appendix B). Consequently the SYK spin liquid can be regarded as a gapless quantum spin liquid with fractionalized fermionic spinons. The crossover to the spin glass phase is induced by the  $q_{EA}$  term in (5.1), which turns out to be identical to the influence of the  $t$  term in the  $t$ - $J$  models of Refs. [51,55]. The latter  $t$  term is known to break the U(1) gauge symmetry, and therefore, by Higgs-confinement continuity, we can regard the low frequency regime of our quantum magnet as a confining regime of the U(1) gauge symmetry. It is also interesting to compare with the analysis of the quantum magnet using bosonic spinons in Refs. [22,23]: that model also exhibits a fractionalized spin liquid regime, and spin glass order appears by the condensation of bosonic spinons, which explicitly higgses the U(1) gauge symmetry (see Appendix A). Moreover the dynamic spectrum  $\chi''(\omega) \sim \omega$  appears not only for bosonic and fermionic spinons in the spin glass regime, but also for the Ising and rotor spin glasses [31,38,41] where there is no fractionalization at any frequency scale. So, as we noted in Sec. I, the random quantum magnet analyzed here yields a realization of fermion-boson duality, and a solvable theory of deconfinement-confinement crossover in a gapless system with finite density matter. We are not aware of other solvable examples of such phenomena.

In Sec. VI, we employed the insights gained from the structure of the spin glass state to make some general remarks on the complexity of infinite-range quantum spin glasses in the low temperature limit. Our main result was that the complexity is generically nonzero and extensive in the limit of vanishing temperature. For the random quantum magnets considered here, the  $SU(M \rightarrow \infty)$  models have a quantum spin liquid ground state with a nonzero extensive entropy in the limit of vanishing temperature [23] (here “extensive” refers to proportionality to  $N$ , the number of sites, and not to  $M$ ). For finite  $M$ , we have shown that this entropy is quenched at an energy scale  $\omega_*$ . Below  $\omega_*$ , we obtain a spin glass state which in the limit of vanishing temperature has no extensive entropy but an extensive complexity. It appears that the chaotic quantum dynamics in the exponentially large phase space explored by the quantum spin liquid gets turned off at low temperatures, and the phase space fragments into an exponentially large number of subspaces. It would be interesting to explore this idea in the context of the holographic  $n\text{AdS}_2/n\text{CFT}_1$  paradigm, which gives a gravitational interpretation of the low-energy Schwarzsian sector describing the quantum spin liquid phase at strong coupling [11,56]: moti-

vated by the existence of landscapes of multi-centered black hole solutions in four dimensional supergravity [57,58], it was previously suggested [31,35–37] that the spin glass crossover could be realized gravitationally in terms of the fragmentation instability of  $\text{AdS}_2$  space-times [34]. The latter gives rise to a landscape of asymptotically  $\text{AdS}_2$  geometries characterized by the number, location, and charge of fragmented throats. It might then be possible to interpret the complexity of the spin glass state as a measure of the volume of the moduli space of gravitational solutions.

## ACKNOWLEDGMENTS

We thank Tom Banks, Debanjan Chowdhury, Antoine Georges, Darshan Joshi, Chenyuan Li, Juan Maldacena, Olivier Parcollet, Henry Shackleton, Grigory Tarnopolsky, Maria Tikhonovskaya, and Alexander Wietek for helpful discussions. This research was supported by the National Science Foundation under Grant No. DMR-2002850. This work was also supported by the Simons Collaboration on Ultra-Quantum Matter, which is a grant from the Simons Foundation (651440, S.S.). F.H. is supported by the U.S. Department of Energy, Office of Science, Office of High Energy Physics under Award Number DE-SC0009988, and by the Paul Dirac and Sivian Funds.

## APPENDIX A: BOSONIC SPINONS

Appendix briefly reviews the bosonic spinon theory of the spin glass state [22,23] of (2.1).

Each site now contains states corresponding to the *symmetric* product of  $\kappa M$  (integer) fundamentals, and (2.2) is replaced by

$$S_\beta^\alpha(i) = b_\beta^\dagger(i)b^\alpha(i) - \kappa\delta_\beta^\alpha, \quad \sum_\alpha b_\alpha^\dagger(i)b^\alpha(i) = \kappa M \quad (\text{A1})$$

with bosons  $b^\alpha(i)$  on each site  $i$ . The bosonic and fermionic spinon models co-incide only for the  $SU(2)$  case of physical interest, with  $M = 2$  and  $\kappa = k = 1/2$ .

Now the perfectly ordered spin-glass has  $\kappa M$  bosons in the  $\alpha = 1$  state (say), and this replaces the bound in (2.17) by

$$q_{EA} \leq \frac{\kappa^2(M-1)}{M}. \quad (\text{A2})$$

Note that (2.17) and (A2) agree for the  $SU(2)$  case. However, unlike (2.17), the bound in (A2) does not vanish in the  $M \rightarrow \infty$  limit, and so spin glass order can be order unity in  $M = \infty$  theory. This order is realized by a Higgs condensate of the bosonic spinons [22,23]

$$\langle b^\alpha \rangle = \sqrt{M}(q_{EA})^{1/4}\delta_{\alpha,1}. \quad (\text{A3})$$

This condensate breaks the U(1) gauge symmetry associated with the bosonic analog of (A1). In the replica theory, condensate requires replica off-diagonal components in the boson Green’s function  $G_{ab}$  at zero frequency [22,23]

$$G_{ab}(i\omega_n) = \delta_{ab}G(i\omega_n) + \beta\delta_{\omega_n,0}g_{ab}. \quad (\text{A4})$$

The replica off-diagonal components of  $g_{ab}$  break replica symmetry, and this symmetry breaking has to satisfy a marginal stability criterion to obtain a gapless boson spectrum.

**APPENDIX B: U(1) GAUGE INVARIANCE**

Consider the following gauge transformation:

$$\begin{aligned} f_a^\alpha(\tau) &\longrightarrow e^{i\phi(\tau)} f_a^\alpha(\tau), & f_{a\alpha}^\dagger(\tau) &\longrightarrow e^{-i\phi(\tau)} f_{a\alpha}^\dagger(\tau), \\ \lambda_a(\tau) &\longrightarrow \lambda_a(\tau) - \partial_\tau \phi. \end{aligned} \quad (\text{B1})$$

This is an invariance of the fermionic formulation of the theory, e.g., (2.4). In the  $G$ - $\Sigma$  formulation (2.13), one can see that the action is invariant under the following transformations:

$$\begin{aligned} G_{ab}(\tau, \tau') &\longrightarrow e^{i[\phi(\tau) - \phi(\tau')]} G_{ab}(\tau, \tau'), \\ \Sigma_{ab}(\tau, \tau') &\longrightarrow e^{i[\phi(\tau) - \phi(\tau')]} \Sigma_{ab}(\tau, \tau'), \\ \lambda_a(\tau) &\longrightarrow \lambda_a(\tau) - \partial_\tau \phi. \end{aligned} \quad (\text{B2})$$

We can use this gauge symmetry to make  $\lambda_a$  time-independent, but cannot remove it entirely because of the periodicity condition on the fields.

**APPENDIX C: HIGHER ORDERS IN  $1/M$** 

In this Appendix, we compute higher orders in the  $1/M$  expansion of the free energy.

We first clarify some notation: we use a matrix dot product both for fields with two and with four indices. Every ‘‘matrix’’ multiplication always involves half of the available indices. Relevant quantities occurring below are

$$\begin{aligned} \delta \Sigma &\equiv \delta \Sigma_{ab}(\tau_1, \tau_2), & \mathbf{G}_Q &\equiv G_Q(\tau_{12}) \delta_{ab}, \\ \mathbf{K} &\equiv K_{ab;cd}(\tau_1, \tau_2; \tau_3, \tau_4). \end{aligned} \quad (\text{C1})$$

These multiply as follows:

$$\begin{aligned} \delta \Sigma \cdot \mathbf{G}_Q &= \int d\tau_3 \sum_c \delta \Sigma_{ac}(\tau_1, \tau_3) (G_Q(\tau_{32}) \delta_{cb}), \\ \mathbf{K} \cdot \mathbf{K} &= \int d\tau_5 d\tau_6 \sum_{ef} K_{ab;ef}(\tau_1, \tau_2; \tau_5, \tau_6) K_{ef;cd} \\ &\quad \times (\tau_5, \tau_6; \tau_3, \tau_4). \end{aligned} \quad (\text{C2})$$

Let us now explain the  $1/M$  expansion of the free energy. We need to consider higher powers of  $\delta \Sigma_{ab}$  in the expansion of  $I[Q]$ . From (2.13), we find that such terms originate from expanding the logarithm:

$$\begin{aligned} -\ln \det \{-\delta'(\tau - \tau') \delta_{ab} - (\Sigma_{ab}(\tau, \tau') + \delta \Sigma_{ab}(\tau, \tau'))\} \\ = \dots + \frac{1}{3} \text{Tr}(\delta \Sigma \cdot \mathbf{G}_Q)^3 + \frac{1}{4} \text{Tr}(\delta \Sigma \cdot \mathbf{G}_Q)^4 + \mathcal{O}(\delta \Sigma^5). \end{aligned} \quad (\text{C3})$$

where we omitted constant, linear and quadratic terms, which are already taken care of. In the functional integral over  $(\delta G_{ab}, \delta \Sigma_{ab})$ , we include these higher order terms by introducing a bilocal source  $J_{ab}$  for  $\delta \Sigma_{ab}$  in the integral (4.2):

$$\begin{aligned} \mathcal{Z}_f[Q] &\propto \exp \left[ - \sum_{k \geq 3} \frac{M}{k} \text{Tr} \left( \frac{\delta}{\delta \mathbf{J}} \right)^k \right]_{\mathbf{J}=0} \\ &\quad \times \int \mathcal{D}[\delta \mathbf{X}] e^{-\frac{M}{2} \delta \mathbf{X}^T \cdot \mathbf{A} \cdot \delta \mathbf{X} + \text{Tr}[\mathbf{J} \cdot \delta \Sigma \cdot \mathbf{G}_Q]} \end{aligned}$$

$$\begin{aligned} &\propto [\det(\mathbf{K} - \mathbf{1})]^{-\frac{1}{2}} \exp \left[ - \sum_{k \geq 3} \frac{M}{k} \text{Tr} \left( \frac{\delta}{\delta \mathbf{J}} \right)^k \right]_{\mathbf{J}=0} \\ &\quad \times \exp \left[ \frac{1}{M} W_Q[\mathbf{J}] \right], \end{aligned} \quad (\text{C4})$$

where we discarded the leading contribution obtained by evaluating  $\mathcal{Z}_f$  on the large  $M$  saddle point, and we defined

$$\begin{aligned} W_Q[\mathbf{J}] &\equiv - \frac{J^2}{2} \int d\tau_1 \dots d\tau_6 \sum_{a,b,c,d} J_{ab}(\tau_1, \tau_2) J_{cd}(\tau_3, \tau_4) Q_{cd} \\ &\quad \times (\tau_6, \tau_4) G_Q(\tau_{15}) G_Q(\tau_{36}) (\mathbf{1} - \mathbf{K})_{ab;cd}^{-1}(\tau_2, \tau_5; \tau_6, \tau_4) \end{aligned} \quad (\text{C5})$$

In order to compute the subleading contributions to the free energy, we need to evaluate the new contributions to  $-\ln \mathcal{Z}_f[Q]$ , which are generated by derivatives with respect to  $\mathbf{J}$ . Note that the logarithm does not simply remove the exponential in (C4) due to the structure of contractions. For instance, the terms involving four and six  $\mathbf{J}$  derivatives take the following form:

$$\begin{aligned} -\ln \mathcal{Z}_f[Q] &= \dots + \left\{ \frac{1}{8M} \text{Tr} \left( \frac{\delta}{\delta \mathbf{J}} \right)^4 W_Q^2 + \left( \frac{1}{36M^2} \text{Tr} \left( \frac{\delta}{\delta \mathbf{J}} \right)^6 \right. \right. \\ &\quad \left. \left. - \frac{1}{108M} \left[ \text{Tr} \left( \frac{\delta}{\delta \mathbf{J}} \right)^3 \right]^2 \right) W_Q^3 + \dots \right\}. \end{aligned} \quad (\text{C6})$$

It is most useful to think about these expressions diagrammatically: the  $\mathbf{J}$ -derivatives produce different Wick contractions among the powers of  $\mathbf{K}$ . For instance, at  $\mathcal{O}(M^{-1})$  we obtain the following contribution to the free energy from the first term in (C6):

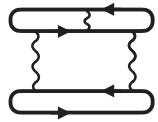
$$\begin{aligned} \text{Diagram} &\propto \frac{J^4}{M} \int d\tau_1 d\tau_2 d\tau_3 d\tau_4 \sum_a Q_{aa}(\tau_{13}) Q_{aa}(\tau_{24}) R_Q^{(4)} \\ &\quad \times (\tau_{14}, \tau_{43}, \tau_{32}) \end{aligned} \quad (\text{C7})$$

Similarly, the last term shown in (C6) gives further contributions at  $\mathcal{O}(M^{-1})$ .

$$\begin{aligned} \text{Diagram} &\propto \frac{J^6}{M} \int d\tau_1 \dots d\tau_6 \sum_{a,b,c} Q_{ab}(\tau_{12}) Q_{bc}(\tau_{34}) Q_{ca} \\ &\quad \times (\tau_{56}) R_Q^{(2)}(\tau_{23}) R_Q^{(2)}(\tau_{45}) R_Q^{(2)}(\tau_{61}) \end{aligned} \quad (\text{C8})$$

At  $\mathcal{O}(M^{-2})$ , we get cubic terms such as the following from the second term shown in (C6):

$$\begin{aligned} \text{Diagram} &\propto \frac{J^6}{M^2} \int d\tau_1 \dots d\tau_6 \sum_{a,b} Q_{ab}(\tau_{14}) Q_{ab}(\tau_{25}) Q_{ab} \\ &\quad \times (\tau_{36}) R_Q^{(3)}(\tau_{15}, \tau_{53}) R_Q^{(3)}(\tau_{42}, \tau_{26}), \end{aligned}$$



$$\propto \frac{J^6}{M^2} \int d\tau_1 \cdots d\tau_6 \sum_{a,b} Q_{ab}(\tau_{13}) Q_{aa}(\tau_{25}) Q_{ab}(\tau_{46}) R_Q^{(2)}(\tau_{14}) R_Q^{(4)}(\tau_{32}, \tau_{26}, \tau_{65}). \quad (\text{C9})$$

We can now see how further potentially divergent terms are generated in the free energy functional at higher orders in  $1/M$ . For example, the diagram (C8) and the last diagram shown in (C9) lead to new contributions to the free energy, which are cubic in the spin glass parameters:

$$\mathcal{F}_{sg} \supset -\frac{e_3}{3} \beta^2 \left( \bar{q}^3 + 3\bar{q} \frac{\text{Tr}q^2}{n} + \frac{\text{Tr}q^3}{n} \right) - e'_3 \beta \bar{q} \times \left( \bar{q}^2 + \frac{\text{Tr}q^2}{n} \right) + \dots, \quad (\text{C10})$$

where  $e_3 = \mathcal{O}(M^{-1})$  and  $e'_3 = \mathcal{O}(M^{-2})$ . All possible terms in the Landau functional theory (e.g., Ref. [38]) are generated systematically this way. The other diagrams shown above give  $1/M$  corrections to the coefficients  $c_i$  and  $d_i$  that we already included in (4.11).

Note that the free energy contribution proportional to  $e_3$  is naively quadratically divergent as  $\beta \rightarrow \infty$ . However, upon using the replica symmetric ansatz for  $q_{ab}$  and the extremization condition (4.23), this divergence is again cured and we obtain a finite limit. This follows from the identity

$$\bar{q}^3 + 3\bar{q} \frac{\text{Tr}q^2}{n} + \frac{\text{Tr}q^3}{n} \longrightarrow \bar{q}^3 - 3\bar{q} q_{EA}^2 + 2q_{EA}^3 \quad (\text{C11})$$

for the replica symmetric ansatz as  $n \rightarrow 0$ .

- 
- [1] M. Frachet, I. Vinograd, R. Zhou, S. Benhabib, S. Wu, H. Mayaffre, S. Krämer, S. K. Ramakrishna, A. P. Reyes, J. Debray, T. Kurosawa, N. Momono, M. Oda, S. Komiya, S. Ono, M. Horio, J. Chang, C. Proust, D. LeBoeuf, and M.-H. Julien, Hidden magnetism at the pseudogap critical point of a cuprate superconductor, *Nat. Phys.* **16**, 1064 (2020).
- [2] Q. Ma, E. M. Smith, Z. W. Cronkwright, M. Dragomir, G. Mitchell, A. I. Kolesnikov, M. B. Stone, and B. D. Gaulin, Dynamic Parallel Spin Stripes from the  $1/8$  anomaly to the End of Superconductivity in  $\text{La}_{1.6-x}\text{Nd}_{0.4}\text{Sr}_x\text{CuO}_4$ , [arXiv:2109.11570](https://arxiv.org/abs/2109.11570).
- [3] S.-D. Chen, M. Hashimoto, Y. He, D. Song, K.-J. Xu, J.-F. He, T. P. Devereaux, H. Eisaki, D.-H. Lu, J. Zaanen, and Z.-X. Shen, Incoherent strange metal sharply bounded by a critical doping in  $\text{Bi2212}$ , *Science* **366**, 1099 (2019).
- [4] R.-H. He, M. Hashimoto, H. Karapetyan, J. D. Koralek, J. P. Hinton, J. P. Testaud, V. Nathan, Y. Yoshida, H. Yao, K. Tanaka, W. Meevasana, R. G. Moore, D. H. Lu, S. K. Mo, M. Ishikado, H. Eisaki, Z. Hussain, T. P. Devereaux, S. A. Kivelson, J. Orenstein, et al., From a Single-Band Metal to a High-Temperature Superconductor via Two Thermal Phase Transitions, *Science* **331**, 1579 (2011).
- [5] Y. Fang, G. Grissonnanche, A. Legros, S. Verret, F. Laliberte, C. Collignon, A. Ataei, M. Dion, J. Zhou, D. Graf, M. J. Lawler, P. Goddard, L. Taillefer, and B. J. Ramshaw, Fermi surface transformation at the pseudogap critical point of a cuprate superconductor, [arXiv:2004.01725](https://arxiv.org/abs/2004.01725).
- [6] E. Mascot, A. Nikolaenko, M. Tikhonovskaya, Y.-H. Zhang, D. K. Morr, and S. Sachdev, Electronic spectra with paramagnon fractionalization in the single band Hubbard model, [arXiv:2111.13703](https://arxiv.org/abs/2111.13703).
- [7] Y.-H. Zhang and S. Sachdev, From the pseudogap metal to the Fermi liquid using ancilla qubits, *Phys. Rev. Research* **2**, 023172 (2020).
- [8] B. Dalla Piazza, M. Mourigal, N. B. Christensen, G. J. Nilsen, P. Tregenna-Piggott, T. G. Perring, M. Enderle, D. F. McMorrow, D. A. Ivanov, and H. M. Rønnow, Fractional excitations in the square-lattice quantum antiferromagnet, *Nat. Phys.* **11**, 62 (2015).
- [9] D. Chowdhury, A. Georges, O. Parcollet, and S. Sachdev, Sachdev-Ye-Kitaev Models and Beyond: A Window into Non-Fermi Liquids, [arXiv:2109.05037](https://arxiv.org/abs/2109.05037).
- [10] S. Sachdev and J. Ye, Gapless Spin-Fluid Ground State in a Random Quantum Heisenberg Magnet, *Phys. Rev. Lett.* **70**, 3339 (1993).
- [11] A. Y. Kitaev, Talks at KITP, University of California, Santa Barbara, entanglement in strongly-correlated quantum matter (2015), <https://online.kitp.ucsb.edu/online/entangled15/>.
- [12] S. Sachdev, Bekenstein-Hawking Entropy and Strange Metals, *Phys. Rev. X* **5**, 041025 (2015).
- [13] Y. Gu, A. Kitaev, S. Sachdev, and G. Tarnopolsky, Notes on the complex Sachdev-Ye-Kitaev model, *J. High Energy Phys.* **02** (2020) 157.
- [14] M. Tikhonovskaya, H. Guo, S. Sachdev, and G. Tarnopolsky, Excitation spectra of quantum matter without quasiparticles I: Sachdev-Ye-Kitaev models, *Phys. Rev. B* **103**, 075141 (2021).
- [15] D. R. Grempel and M. J. Rozenberg, Fluctuations in a Quantum Random Heisenberg Paramagnet, *Phys. Rev. Lett.* **80**, 389 (1998).
- [16] L. Arrachea and M. J. Rozenberg, Infinite-range quantum random Heisenberg magnet, *Phys. Rev. B* **65**, 224430 (2002).
- [17] H. Shackleton, A. Wietek, A. Georges, and S. Sachdev, Quantum Phase Transition at Nonzero Doping in a Random  $t$ - $J$  Model, *Phys. Rev. Lett.* **126**, 136602 (2021).
- [18] G. Gur-Ari, R. Mahajan, and A. Vaezi, Does the SYK model have a spin glass phase? *J. High Energy Phys.* **11** (2018) 070.
- [19] D. G. Joshi and S. Sachdev, Anomalous density fluctuations in a random  $t$ - $J$  model, *Phys. Rev. B* **102**, 165146 (2020).
- [20] M. Mitrano, A. A. Husain, S. Vig, A. Kogar, M. S. Rak, S. I. Rubeck, J. Schmalian, B. Uchoa, J. Schneeloch, R. Zhong, G. D. Gu, and P. Abbamonte, Anomalous density fluctuations in a strange metal, *Proc. Natl. Acad. Sci. USA* **115**, 5392 (2018).
- [21] A. A. Husain, M. Mitrano, M. S. Rak, S. Rubeck, B. Uchoa, K. March, C. Dwyer, J. Schneeloch, R. Zhong, G. D. Gu, and P. Abbamonte, Crossover of charge fluctuations across the strange metal phase diagram, *Phys. Rev. X* **9**, 041062 (2019).
- [22] A. Georges, O. Parcollet, and S. Sachdev, Mean Field Theory of a Quantum Heisenberg Spin Glass, *Phys. Rev. Lett.* **85**, 840 (2000).

- [23] A. Georges, O. Parcollet, and S. Sachdev, Quantum fluctuations of a nearly critical Heisenberg spin glass, *Phys. Rev. B* **63**, 134406 (2001).
- [24] C. Wang, A. Nahum, M. A. Metlitski, C. Xu, and T. Senthil, Deconfined quantum critical points: symmetries and dualities, *Phys. Rev. X* **7**, 031051 (2017).
- [25] A. Thomson and S. Sachdev, Fermionic Spinon Theory of Square Lattice Spin Liquids near the Néel State, *Phys. Rev. X* **8**, 011012 (2018).
- [26] R. Monasson, Structural Glass Transition and the Entropy of the Metastable States, *Phys. Rev. Lett.* **75**, 2847 (1995).
- [27] S. Franz and G. Parisi, Effective potential in glassy systems: theory and simulations, *Physica A* **261**, 317 (1998).
- [28] M. Mézard and G. Parisi, Thermodynamics of glasses: a first principles computation, *J. Phys.: Condens. Matter* **11**, A157 (1999).
- [29] F. Zamponi, Mean field theory of spin glasses, [arXiv:1008.4844](https://arxiv.org/abs/1008.4844).
- [30] C. De Dominicis and I. Giardinà, *Random Fields and Spin Glasses: A Field Theory Approach* (Cambridge University Press, Cambridge, UK, 2006).
- [31] T. Anous and F. M. Haehl, The quantum  $p$ -spin glass model: A user manual for holographers, *J. Stat. Mech.* (2021) 113101.
- [32] S. Sachdev, Holographic metals and the fractionalized Fermi liquid, *Phys. Rev. Lett.* **105**, 151602 (2010).
- [33] J. Maldacena and D. Stanford, Remarks on the Sachdev-Ye-Kitaev model, *Phys. Rev. D* **94**, 106002 (2016).
- [34] J. M. Maldacena, J. Michelson, and A. Strominger, Anti-de Sitter fragmentation, *J. High Energy Phys.* **02** (1999) 011.
- [35] D. Anninos, T. Anous, J. Barandes, F. Denef, and B. Gaasbeek, Hot Halos and Galactic Glasses, *J. High Energy Phys.* **01** (2012) 003.
- [36] D. Anninos, T. Anous, F. Denef, and L. Peeters, Holographic Vitrification, *J. High Energy Phys.* **04** (2015) 027.
- [37] D. Anninos, T. Anous, and F. Denef, Disordered Quivers and Cold Horizons, *J. High Energy Phys.* **12** (2016) 071.
- [38] N. Read, S. Sachdev, and J. Ye, Landau theory of quantum spin glasses of rotors and Ising spins, *Phys. Rev. B* **52**, 384 (1995).
- [39] A. Kitaev and S. J. Suh, The soft mode in the Sachdev-Ye-Kitaev model and its gravity dual, *J. High Energy Phys.* **05** (2018) 183.
- [40] J. Ye, S. Sachdev, and N. Read, Solvable Spin Glass of Quantum Rotors, *Phys. Rev. Lett.* **70**, 4011 (1993).
- [41] L. F. Cugliandolo, D. R. Grempel, and C. A. da Silva Santos, From Second to First Order Transitions in a Disordered Quantum Magnet, *Phys. Rev. Lett.* **85**, 2589 (2000).
- [42] N. Read and D. M. Newns, On the solution of the Coqblin-Schrieffer Hamiltonian by the large- $N$  expansion technique, *J. Phys. C: Solid State Phys.* **16**, 3273 (1983).
- [43] A. V. Chubukov, S. Sachdev, and J. Ye, Theory of two-dimensional quantum Heisenberg antiferromagnets with a nearly critical ground state, *Phys. Rev. B* **49**, 11919 (1994).
- [44] A. J. Bray and M. A. Moore, Replica theory of quantum spin glasses, *J. Phys. C* **13**, L655 (1980).
- [45] P. Anders, E. Gull, L. Pollet, M. Troyer, and P. Werner, Dynamical Mean Field Solution of the Bose-Hubbard Model, *Phys. Rev. Lett.* **105**, 096402 (2010).
- [46] O. Akerlund, P. de Forcrand, A. Georges, and P. Werner, Dynamical Mean Field Approximation Applied to Quantum Field Theory, *Phys. Rev. D* **88**, 125006 (2013).
- [47] O. Akerlund, P. de Forcrand, A. Georges, and P. Werner, Extended Mean Field study of complex  $\phi^4$ -theory at finite density and temperature, *Phys. Rev. D* **90**, 065008 (2014).
- [48] Q. Si, S. Rabello, K. Ingersent, and J. L. Smith, Locally critical quantum phase transitions in strongly correlated metals, *Nature (London)* **413**, 804 (2001).
- [49] J.-X. Zhu, D. R. Grempel, and Q. Si, Continuous Quantum Phase Transition in a Kondo Lattice Model, *Phys. Rev. Lett.* **91**, 156404 (2003).
- [50] J.-X. Zhu, S. Kirchner, R. Bulla, and Q. Si, Zero-Temperature Magnetic Transition in an Easy-Axis Kondo Lattice Model, *Phys. Rev. Lett.* **99**, 227204 (2007).
- [51] O. Parcollet and A. Georges, Non-Fermi-liquid regime of a doped Mott insulator, *Phys. Rev. B* **59**, 5341 (1999).
- [52] X.-Y. Song, C.-M. Jian, and L. Balents, Strongly Correlated Metal Built from Sachdev-Ye-Kitaev Models, *Phys. Rev. Lett.* **119**, 216601 (2017).
- [53] G. Parisi, Infinite Number of Order Parameters for Spin-Glasses, *Phys. Rev. Lett.* **43**, 1754 (1979).
- [54] K. Fischer and J. Hertz, *Spin Glasses*, Cambridge Studies in Magnetism (Cambridge University Press, Cambridge, UK, 1993).
- [55] D. G. Joshi, C. Li, G. Tarnopolsky, A. Georges, and S. Sachdev, Deconfined critical point in a doped random quantum Heisenberg magnet, *Phys. Rev. X* **10**, 021033 (2020).
- [56] J. Maldacena, D. Stanford, and Z. Yang, Conformal symmetry and its breaking in two dimensional nearly anti-de-Sitter space, *PTEP* **2016**, 12C104 (2016).
- [57] F. Denef, Supergravity flows and D-brane stability, *J. High Energy Phys.* **08** (2000) 050.
- [58] B. Bates and F. Denef, Exact solutions for supersymmetric stationary black hole composites, *J. High Energy Phys.* **11** (2011) 127.